Study on the influence of wave-shaper dimensions on the penetration performance of a 125-mm shaped charge warhead

Tran Van De*, Nguyen The Duy, Nguyen Dinh Linh

Institute of Missile, Academy of Military Science and Technology, 17 Hoang Sam, Nghia Do, Hanoi, Vietnam.

*Corresponding author: trande1025@gmail.com

Received 24 Jun. 2026; Revised 18 Aug. 2026; Accepted 04 Sep. 2026; Published 16 Sep. 2026.

DOI: https://doi.org/10.54939/1859-1043.j.mst.FMC.2026.70-79

ABSTRACT

This paper presents a study on the influence of wave-shaper geometry on the penetration performance of a 125-mm shaped charge warhead. The study investigates different wave-shaper dimensions, including diameter and thickness, and evaluates their effects on the formation and convergence of the detonation wave as well as on the penetration performance against a steel target. Numerical simulations are carried out using ANSYS Autodyn 2D with Eulerian and Lagrangian solvers. The results show that the wave-shaper dimensions alter the detonation-wave front, thereby increasing the jet tip velocity and the penetration depth into a homogeneous steel target.

Keywords: Shaped charge; Detonation wave; Wave interference; Autodyn 2D.

1. INTRODUCTION

Shaped charge warheads play an important role in modern armour-piercing weapons. The performance of a shaped charge warhead is characterized by several parameters, including penetration depth, penetration-hole diameter, jet tip velocity, and jet coherency. To improve the performance of shaped charge warheads, several approaches can be adopted, such as modifying the liner structure, using high-energy explosives, and changing the wave-shaper configuration. Among these approaches, modifying the wave-shaper structure is considered highly effective and relatively simple. Previous domestic and international studies have confirmed that the use of a wave shaper can improve the penetration performance of shaped charge warheads. However, domestic research works still have several limitations. Due to military confidentiality, studies in this field worldwide are rarely published in a comprehensive manner and mainly remain at a qualitative level.

Studies on the influence of wave shapers have mainly been conducted using flat cylindrical wave-shaper models. Meanwhile, many other wave-shaper geometries are used in warheads. Investigating different wave-shaper geometries can help explain the basis for selecting an appropriate wave-shaper configuration for each specific case.

This paper presents a study on the influence of wave-shaper geometry on the penetration performance of a 125-mm shaped charge warhead, carried out using numerical simulation in ANSYS Autodyn. The objective is to investigate the detonation-wave formation process, the variation law of penetration depth, and the influence of geometric parameters, thereby proposing a suitable wave-shaper configuration for a 125-mm warhead to improve practical effectiveness.

2. SIMULATION MODEL

2.1. Formation mechanism of the shaped charge jet and the destruction process of the steel plate

2.1.1. Formation process of the shaped charge jet

Upon initiation, the detonation wave acts on the liner and generates a compressive pressure of up to several million atmospheres. The compression velocity reaches 5÷15 km/s, with an energy density 20÷30 times higher than that of a conventional explosion.

This energy acts intensively mainly on the front surface of the liner. The inner metal layer, accounting for about (10÷20%), moves toward the apex at a much higher velocity than the outer layer. This convergence and velocity gradient stretch the metal into a jet: the inner layer forms the jet tip, while the outer layer forms the slug.

At this stage, the liner deforms and behaves like an ideal incompressible fluid, with very high density and jet tip velocity (5÷15 km/s). The continuous concentrated jet is elongated and supplied with material from the slug. This process terminates only when the ductility limit of the metal can no longer sustain further stretching.

2.1.2. Destruction process of the steel plate by the shaped charge jet

The destruction process of the steel plate by the jet is shown in Figure 1.

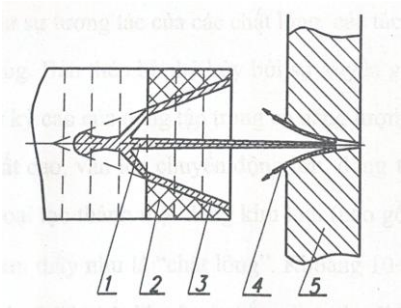


Figure 1. *Schematic diagram of the interaction between the shaped charge jet and the steel plate: 1 - Shaped charge jet; 2 - Explosive; 3 - Liner; 4 - Jet metal and ejected steel debris; 5 - Steel plate*

Under the penetrating action of the concentrated metal jet, the steel plate is destroyed by continuous impact pulses. The concentrated metal jet has an extremely high velocity and energy, with compressive pressure reaching several million atmospheres. Under such severe impact conditions, the bonding forces between the particles of the steel plate can be regarded as extremely small, and the strength of the steel plate becomes negligible. The penetration of the metal jet into the steel plate follows a "flow-in" mechanism, similar to the interaction between fluids, with the process governed by hydrodynamic laws. The steel plate is destroyed by the continuous penetration process under the very high pressure generated by the high-energy concentrated jet. The concentrated jet breaks up the metal particles of the plate into a metallic flow, including very small metal fragments, which are ejected outward through the penetration hole formed by the jet.

2.2. Mathematical model

The investigated model is a 125-mm-diameter shaped charge warhead, consisting of the following components: booster, main explosive charge, wave shaper, liner, and casing. The model is represented in the (XOY) coordinate system, in which the (OX) axis is the axis of symmetry of the warhead and (K) denotes the initiation point. Due to the axial symmetry of the shaped charge warhead, a 2D Euler solver and corresponding material models are used to simulate the propagation of the detonation wave and the formation of the shaped charge jet. In the simulation model, a mesh size of 0,5 mm × 0,5 mm, is used. The interaction between the detonation products and the casing at the boundary of the computational domain is not considered.

To investigate the influence of the wave shaper, different simulation cases are established in which all other components are kept unchanged, while only the wave-shaper structure is varied. This allows the effects of the wave shaper on the detonation wave and the shaped charge jet to be evaluated.

2.3. Material model

2.3.1. Explosive material model

Two types of explosives are used in the simulation model: PENT 1.77 is used as the booster charge, while OCTOL is used as the main explosive charge. Both materials are available in the software material library [4].

For PENT 1.77, point initiation is applied at point (K) (Figure 1). The appropriate material model is described by the JWL (Jones-Wilkins-Lee) equation of state. The JWL equation of state for detonation products is expressed as follows [6]:

$$p = A\left(1-\frac{\omega}{R_1 V}\right)e^{-R_1 V} + B\left(1-\frac{\omega}{R_2 V}\right)e^{-R_2 V} + \frac{\omega E}{V}$$

$$p = A\left(1-\frac{\omega}{R_1 V}\right)e^{-R_1 V} + B\left(1-\frac{\omega}{R_2 V}\right)e^{-R_2 V} + \frac{\omega E}{V}$$

where: p – The pressure of the detonation products; ω, A, B, R1 and R2 - Empirical constants (Table 1, 2), selected from the software material library [1, 4]; V= ρ0/ρ - Ratio of the initial density to the density at the considered calculation time; E – Specific internal energy of the explosive.

Table 1. *JWL equation-of-state parameters of PENT 1.77 explosive.*

ρ_0(g/cm^3)	A(Mbar)	B(Mbar)	R_1	R_2	ω	D(m/s)
1,77	6,17	0,169	4,4	1,2	0,25	8300

Table 2. *JWL equation-of-state parameters of OCTOL explosive.*

ρ_0(g/cm^3)	A(Mbar)	B(Mbar)	R_1	R_2	ω	D(m/s)
1,821	7,49	0,134	4,5	1,2	0,38	8480

2.3.2. Liner material model

The liner material is Cu-OFHC copper, with a density of 8,93 (g.cm^{-3}), Although this material has good ductility, under impact loading and high strain-rate deformation, it is described using the Steinberg-Guinan strength model together with the Shock equation of state.

**) Steinberg-Guinan strength model*

The Steinberg-Guinan strength model was proposed in 1978 to describe material behaviour under very high strain-rate deformation. The shear modulus and yield strength are determined as follows [2]:

$$G = G_0\left\{1+\left(\frac{G_p'}{G_0}\right)\frac{p}{\eta^{1/3}}+\left(\frac{G_T'}{G_0}\right)(T-300)\right\}$$

$$\sigma_c^d = \sigma_c^0\left\{1+\left(\frac{(\sigma_c^d)_P'}{\sigma_c^0}\right)\frac{p}{\eta^{1/3}}+\left(\frac{G_T'}{G_0}\right)(T-300)\right\}(1+\beta\varepsilon_p)^n$$

$$\sigma_c^0(1+\beta\varepsilon_p)^n \le \sigma_{c\,\max}^d$$

where: β, n - Material constants; ε_p - Effective plastic strain; G_0 and σ_c^0 - Shear modulus and yield strength at the reference state (T_0 = 300 K, $p = 0$); G and σ_c^d - The shear modulus and yield strength under dynamic loading; η - Compression ratio v_0 / v; p - Pressure; T - Temperature; $G_p', G_T', \left(\sigma_c^d\right)_p'$ - Derivatives of G and σ_c^d with respect to p, T .

**) Johnson-Cook strength model:*

This model is used to describe the strength behaviour of metallic materials under large deformation, high strain rate, and high temperature when the component is subjected to high-velocity impact loading. In this model, the yield strength varies depending on the strain level, strain rate, and temperature [7].

$$\sigma_c^d = \left[A + B\varepsilon_p^n \right] \left(1 + C \ln \left(\frac{\dot{\varepsilon}_p}{\dot{\varepsilon}_{p0}} \right) \right) \left(1 - \bar{T}^m \right)$$

where: σ_c^d - Dynamic yield strength; A, B, C, m and n - Material constants (A - Yield strength of the material, B - Strain-hardening coefficient, C - Strain-rate constant, m - Thermal softening exponent, n : Strain-hardening exponent); ε_p - Effective plastic strain; $\dot{\varepsilon}_p$ - Effective plastic strain rate; $\dot{\varepsilon}_{p0}$ - Reference effective plastic strain rate, determined experimentally; $\bar{T} = \left(T - T_{room} \right) / \left(T_{nc} - T_{room} \right)$ (T : Material temperature (K), T_{room} : Ambient temperature, T_{nc} Melting temperature of the material).

The Shock equation-of-state parameters and Steinberg-Guinan strength-model parameters of Cu-OFHC copper are given in Tables 3 and 4 [2].

Table 3. *Shock equation-of-state parameters of Cu-OFHC.*

ρ_0 (g/cm^3)	Γ	C_1 ($cm.\mu s^{-1}$)	S_1	C_2 ($cm.\mu s^{-1}$)	S_2	$\frac{VB}{v_0}$	$\frac{VB}{v_0}$
8,96	2,02	0,394	1,489	0	0	0	0

Table 4. *Steinberg-Guinan strength-model parameters of CU-OFCH.*

G (Mbar)	σ_c^0 (Mbar)	$\sigma_{c\ max}^d$ (Mbar)	β	N	$G_T^{'}$	$G_T^{'}$ (Mbar/K)	$\left(\sigma_c^d\right)_p^{'}$	T_{nc} (K)
0,477	0,0012	0,0064	36	0,45	1,35	-1,789e-4	0,003396	1790

2.3.3. Casing material model

The casing material is Steel-1006 with a density of *7,896* (g/cm^3). Under explosive loading, the material undergoes large deformation, leading to changes in both the volume and shape of the elements. Therefore, the Shock equation of state is used to describe the material model of the casing.

The Shock equation-of-state parameters of the casing material are given in Table 5 [2]:

Table 5. *Shock equation-of-state parameters of Steel-1006.*

ρ_0 (g/cm^3)	Γ	C_1 ($cm.\mu s^{-1}$)	S_1	C_2 ($cm.\mu s^{-1}$)	S_2	$\frac{VB}{v_0}$	$\frac{VB}{v_0}$
7,896	2,17	0,4569	1,49	0	0	0	0

2.3.4. Wave-shaper material model

According to [1], the wave-shaper material used in the simulation model for the shaped-charge jet formation process is Plexiglass. The material behavior is described using the Shock equation of state. The Shock equation-of-state parameters of Plexiglass are given in Table 6:

Table 6. *Shock equation-of-state parameters of Plexiglass.*

$\rho_0(g/cm^3)$	Γ	C_1 $(cm.\mu s^{-1})$	S_1	C_2 $(cm.\mu s^{-1})$	S_2	VE / v_0	VB / v_0
1,186	*0,97*	*0,2598*	*1,516*	*0*	*0*	*0*	*0*

2.4. Initial and boundary conditions

Point initiation is used in the simulation, and the initiation location is shown in Figure 2. The FlowOut boundary condition is applied to all boundaries of the computational domain, except for the axis of symmetry. This allows the detonation products and the casing fragments to flow out of the computational domain without interacting with the boundaries.

3. SIMULATION RESULTS

3.1. Model verification

The established model conditions are used to simulate the penetration process of the PG-29V round with a caliber of 105 mm. According to the published tactical and technical specifications, the PG-29V round is capable of penetrating a 600-mm-thick homogeneous steel plate, as verified and reported by experiments.

The simulated penetration-depth result of the PG-29V round is shown in Figure 2.

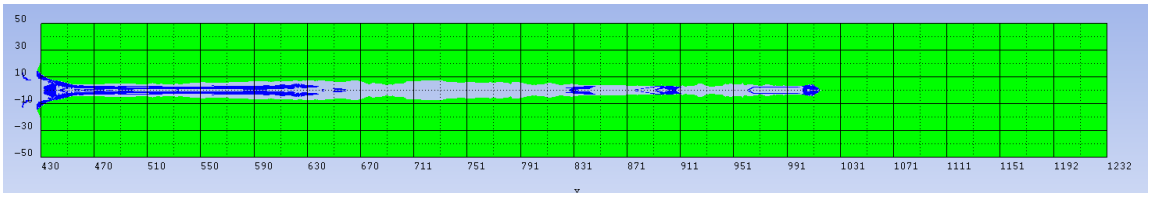


Figure 2. *Penetration-depth result of the PG-29V round.*

Table 7. *Comparison between simulation results and technical specification.*

	Simulation result	**Technical specification**	**Error**
Penetration depth of the PG-29V round (mm)	585	600	2,5%

The simulated penetration depth of the PG-29V round into the steel plate reaches 585 mm, which is close to the published tactical and technical specification. The result shows good agreement between the calculation result obtained from the simulation model developed by the authors and the experimental data. This demonstrates the reliability of the simulation model established in this study, which can be used for subsequent research and calculations.

3.2. Effect of wave-shaper diameter

This section investigates the influence of the wave-shaper diameter on detonation-wave propagation and shaped charge jet formation. The wave shaper is cylindrical, with its thickness kept constant while only its diameter is varied. The wave-shaper thickness (b) is fixed at 28 mm, and the diameter (d) is varied from 54 mm to 78 mm. The investigated wave-shaper diameter cases are given in Table 8.

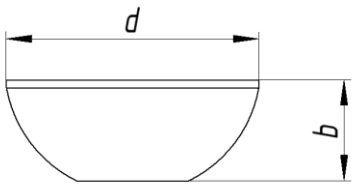


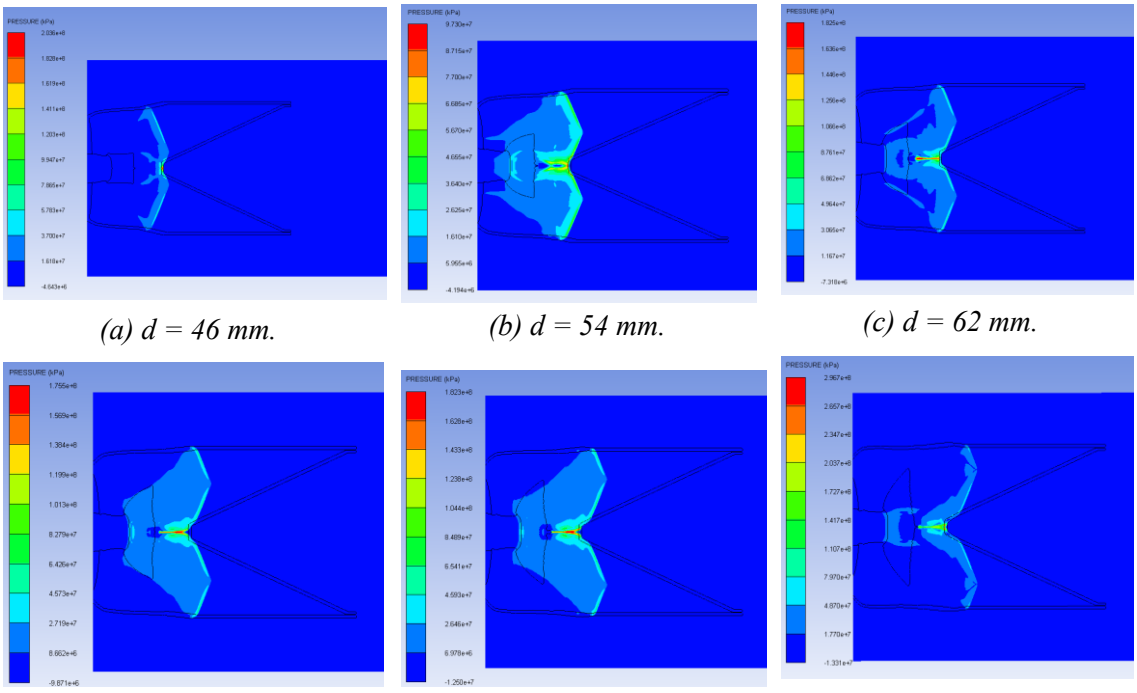
Figure 3. *Wave-shaper geometry used for investigation.*

Table 8. *Wave-shaper diameter variation cases.*

Cases	1	2	3	4	5	5
d (cm)	46	54	62	70	78	86

The investigated jet parameters include jet tip velocity, penetration depth, and the propagation and interaction of the detonation wave with the liner.

Investigation results



(a) d = 46 mm. *(b) d = 54 mm.* *(c) d = 62 mm.*

(d) d = 70 mm. *(e) d = 78 mm.* *(f) d = 86 mm.*

Figure 4. *Detonation-wave front at the moment of interaction with the liner for different wave-shaper diameters.*

The jet tip velocity at a distance equal to twice the explosive charge diameter from the liner mouth for different wave-shaper diameters is presented in table 9 below:

Table 9. *Jet tip velocity for different wave-shaper diameters.*

d (mm)	46	54	62	70	78	86
Jet tip velocity (m/s)	8101,5	8302,4	8413,3	8630,0	9237,4	9016,1

- The penetration-depth results for different wave-shaper diameters are presented in figure 5 and table 10 below

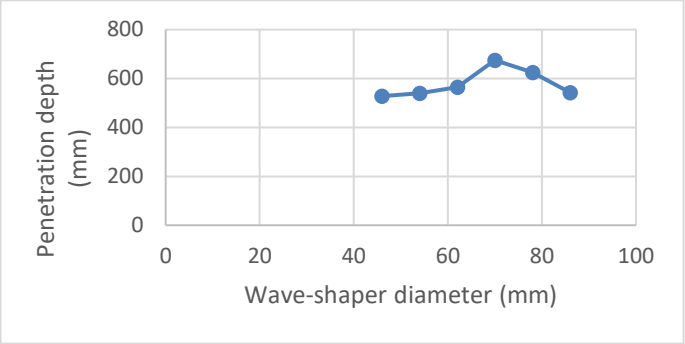


Figure 5. *Variation of penetration depth with wave-shaper diameter.*

Table 10. *Penetration depth versus wave-shaper diameter.*

d (mm)	46	54	62	70	78	86
Penetration depth (mm)	528	540	565	675	625	542

From the investigation results, several remarks can be drawn:

- When the wave-shaper diameter increases from 46 mm to 86 mm, the jet tip velocity at a distance equal to twice the explosive charge diameter gradually increases and reaches its maximum value when the wave-shaper diameter is 78 mm (Table 10). When the diameter continues to increase to 86 mm, the jet tip velocity decreases. This can be explained as follows: as the wave-shaper diameter increases from 46 mm to 78 mm, the detonation wave propagating around the wave shaper reaches the secondary initiation point (T) faster than the wave propagating directly through the wave shaper. As a result, the formed detonation-wave front has a conical shape, and the detonation-wave front compresses the liner surface more uniformly as the wave-shaper diameter increases. When the wave-shaper diameter exceeds 78 mm, the jet tip velocity decreases because the compression angle of the detonation-wave front acting on the liner surface is no longer optimal.

- The penetration-depth results of the jet penetrating the steel target show that, when the wave-shaper diameter increases from 46 mm to 70 mm, the penetration depth increases and reaches its maximum value at a diameter of 70 mm. When the wave-shaper diameter continues to increase to 86 mm, the penetration depth gradually decreases. The variation in penetration depth is caused by the change in jet tip velocity. A higher jet tip velocity corresponds to higher jet penetration energy. However, when the jet tip velocity becomes too high, jet breakup is more likely to occur, thereby reducing the penetration depth despite the high jet tip velocity.

3.3. Effect of wave-shaper thickness

This section investigates the influence of wave-shaper thickness on detonation-wave propagation and shaped charge jet formation. The wave-shaper shape and diameter are kept unchanged, while only its thickness is varied. The wave-shaper diameter is fixed at 70 mm, and the thickness (b) is varied from 10 mm to 50 mm. The investigated wave-shaper thickness cases are given in Table 11.

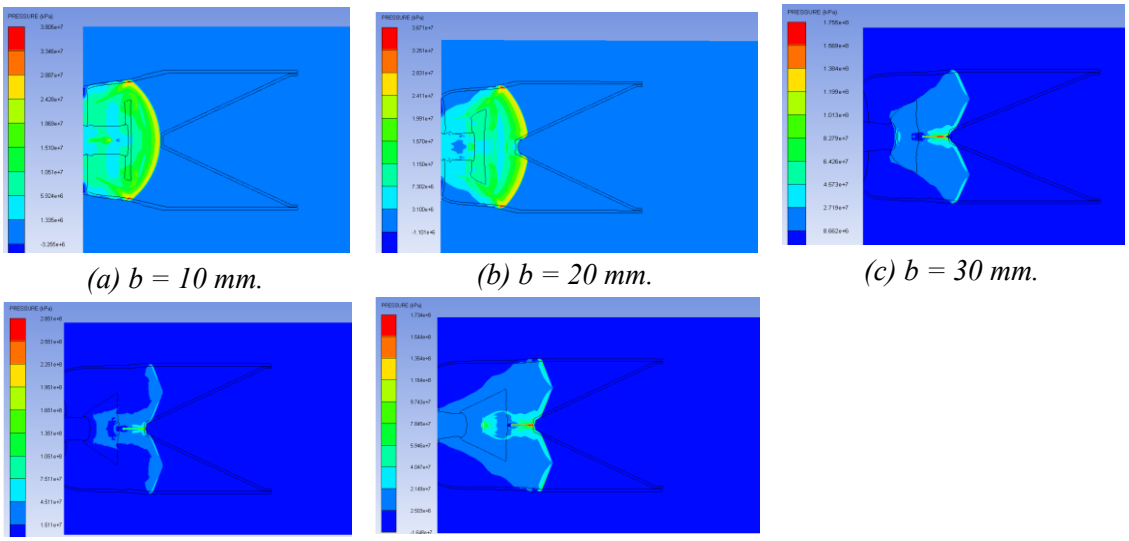
Table 11. *Wave-shaper thickness cases.*

Cases	1	2	3	4	5
b (mm)	10	20	30	40	50

The investigated jet parameters include jet tip velocity, penetration depth, and the propagation

and interaction of the detonation wave with the liner.

Investigation results



(a) b = 10 mm. *(b) b = 20 mm.* *(c) b = 30 mm.*

(d) b = 40 mm. *(e) b = 50 mm.*

Figure 6. *Detonation-wave front at the moment of interaction with the liner for different wave-shaper thicknesses.*

The jet tip velocity at a distance equal to twice the explosive charge diameter from the liner mouth for different wave-shaper thicknesses is presented in the table 12 below:

Table 12. *Jet tip velocity for different wave-shaper thicknesses.*

b (mm)	10	20	30	40	50
Jet tip velocity (m/s)	8101,5	8302,4	8630,0	8688,0	8748,0

- The penetration-depth results for different wave-shaper thicknesses are presented in Figure 7 and Table 13.

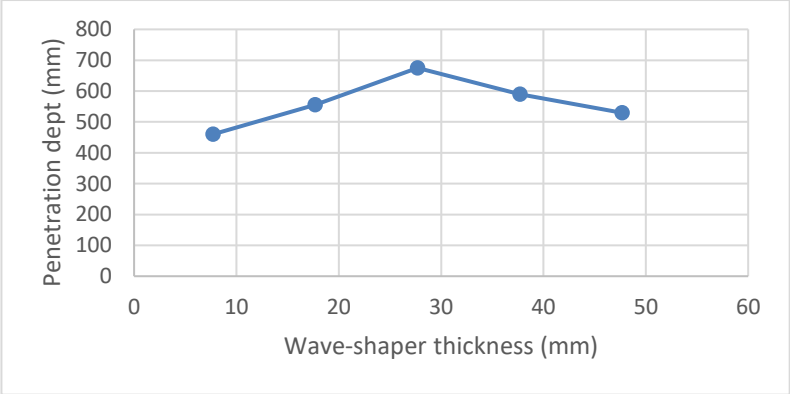


Figure 7. *Variation of penetration depth with wave-shaper thickness.*

Table 13. *Penetration-depth results for different wave-shaper thicknesses.*

b (mm)	10	20	30	40	50
Penetration depth (mm)	460	555	675	590	530

From the investigation results, several remarks can be drawn:

- As the wave-shaper thickness b increases from 10 mm to 50 mm, the jet tip velocity also increases. The penetration depth increases when b increases from 10 mm to 30 mm; however, when b further increases from 30 mm to 50 mm, the penetration depth decreases.

This can be explained as follows:

- When b = 10 mm and b = 20 mm, the shock wave propagating through the wave shaper initiates the explosive behind the wave shaper. Therefore, the formed wave front remains spherical due to the direct propagation of the detonation wave through the wave shaper.

- When b > 30 mm, the detonation wave cannot propagate through the wave shaper. The wave front formed behind the wave shaper is generated by the wave propagating from the secondary initiation point. Behind the wave shaper, wave interference occurs, producing a high-pressure region that compresses the liner. As the thickness b increases, the wave-shaping effect becomes stronger, the explosive region behind the wave shaper is less affected by the detonation wave passing through the wave shaper, and the influence of wave interference becomes more pronounced. As a result, the jet tip velocity increases.

According to the penetration-depth results, the penetration depth increases as the wave-shaper thickness increases from 10 mm to 30 mm and reaches its maximum value at b = 30 mm. When the wave-shaper thickness continues to increase to 40 mm and 50 mm, the penetration depth decreases. As the wave-shaper thickness increases, the wave-shaping effect becomes stronger, producing wave interference that increases the pressure acting on the liner, thereby increasing the jet tip velocity and, consequently, the penetration depth. However, when the jet tip velocity becomes too high, jet breakup may occur, reducing the penetration effectiveness of the jet.

4. CONCLUSIONS

The simulation results are consistent with the theoretical analysis. The results indicate that, when the wave-shaper diameter and thickness are varied, the penetration depth first tends to increase and then gradually decreases.

The wave shaper has a clear influence on the detonation-wave formation process behind the wave shaper, thereby affecting the penetration depth. The combined wave front, formed by the two wave sources propagating around the wave shaper and directly through the wave shaper, acts on the liner element region that forms the jet tip and produces the greatest penetration depth. In the case of Mach-wave interference, a localized high-pressure region with high velocity appears; however, the penetration performance is not high due to jet breakup.

The study results show that the geometric parameters of the wave shaper, including thickness and diameter, affect the detonation-wave formation process and the penetration depth of a 125-mm shaped charge warhead. This provides a basis for calculating and designing a wave shaper for a 125-mm shaped charge warhead.

The study on the influence of the wave shaper on the penetration depth of a 125-mm shaped charge warhead also indicates that several issues require further investigation:

- Investigation of the influence of wave-shaper geometry and material on the penetration depth of shaped charge warheads.

- Investigation of methods for determining suitable wave-shaper parameters for shaped charge warheads.

REFERENCES

[1]. Nguyen Dinh Linh, Le Hai Thuong, and Nguyen Xuan Thanh, *"Optimization of structural parameters of the warhead to the penetration ability of the shaped charge"*, JMST, no. FEE, pp. 212–218, (2024).

[2]. ANSYS, *"Autodyn User's Manual"*, http://www.ansys.com, (2021).
[3]. ANSYS, Inc, *"ANSYS Workbench User's Guide"*, (2011).
[4]. ANSYS, Inc, *"Introduction to ANSYS Explicit Dynamics"*, (2011).
[5]. Zhe Wang, Jian-Wei Jiang, Shu-You Wang & Han Liu, *"Jet Formation and Penetration Study of Double-Layer Shaped Chanrge"*, Journal of Energetic Materials, (2017).
[6]. Zu X. D., Huang Z. X., Zhu C. S. and Xiao Q. Q, *"Study of detonation wave contours in EFP warhead"*, Defence technology, (2016).
[7]. Tran Dinh Thanh, Nguyen Van Thuy, Do Van Minh, *"Physics of Explosion and Impact"*, (2022).

TÓM TẮT

Nghiên cứu ảnh hưởng của kích thước tấm chắn sóng đến uy lực xuyên của đầu nổ xuyên lõm cỡ 125 mm

Bài báo trình bày nghiên cứu ảnh hưởng của hình dạng hình học của tấm chắn sóng (TCS) đến uy lực của đầu nổ xuyên lõm cỡ 125 mm. Nghiên cứu tiến hành khảo sát các tham số kích thước TCS khác nhau (đường kính, bề dày) và ảnh hưởng của chúng đến quá trình hình thành, hội tụ sóng nổ và hiệu quả xuyên thép bằng cách sử dụng phương pháp mô phỏng số trên phần mềm ANSYS Autodyn 2D với bộ giải Euler và Lagrange. Kết quả nghiên cứu cho thấy các kích thước TCS làm thay đổi bề mặt sóng nổ, từ đó giúp tăng vận tốc đỉnh dòng xuyên và chiều sâu xuyên phá đối với mục tiêu thép đồng nhất.

Từ khóa: Xuyên lõm; Sóng nổ; Giao thoa sóng; Autodyn 2D.